Enhancement of the Fluorescence of the Blue Fluorescent Proteins by High Pressure or Low Temperature

Koit Mauring,[†] Jason Deich,[‡] Federico I. Rosell,[§] Tim B. McAnaney, W. E. Moerner, and Steven G. Boxer*

Department of Chemistry, Stanford University, Stanford, California 94305-5080

Received: November 9, 2004; In Final Form: March 17, 2005

Green fluorescent proteins bearing the Y66H mutation exhibit strongly blue-shifted fluorescence excitation and emission spectra. However, these blue fluorescent proteins (BFPs) have lower quantum yields of fluorescence ($\Phi_f \sim 0.20$), which is believed to stem from the increased conformational freedom of the smaller chromophore. We demonstrate that suppression of chromophore mobility by increasing hydrostatic pressure or by decreasing temperature can enhance the fluorescence quantum yield of these proteins without significantly affecting their absorption properties or the shape of the fluorescence spectra. Analysis of the fluorescence lifetimes in the picosecond and nanosecond regimes reveals that the enhancement of the fluorescence quantum yield is due to the inhibition of fast quenching processes. Temperature-dependent fluorescence measurements reveal two barriers (~19 and 3 kJ/mol, respectively) for the transition into nonfluorescing states. These steps are probably linked with dissociation of the hydrogen bond between the chromophore and His148 or an intervening water molecule and to the barrier for chromophore twisting in the excited state, respectively. The chromophore's hydrogen-bond equilibrium at room temperature is dominated by entropic effects, while below ~200 K the balance is enthalpy-driven.

Introduction

Considerable efforts have been made over the past 10 years to engineer variants of the green fluorescent protein (GFP) with desirable physicochemical properties for use as genetically encoded protein labels in vivo.[1,2] Some of these changes have yielded variants that are sensitive reporters of environmental conditions (e.g., pH, ion concentration, and redox potential), and others fold and form the chromophore more efficiently at 37 °C. While some modifications have also resulted in proteins with shifted fluorescence (e.g., blue, cyan, yellow, and gold[1,3,4]), the marked reduction in the fluorescence quantum yield of the protein (Φ_f) that accompanies some of these modifications has limited their usage in cellular biology investigations. Similarly, naturally occurring fluoroproteins that emit at longer wavelengths (e.g., *Hc*Red) tend to be weak fluorophores. This shortcoming underscores the importance of identifying the structural factors that are responsible for the bright fluorescence of GFP because such an understanding could lead to the rational optimization of GFP-like proteins that are weakly fluorescent.

The structure of GFP in the immediate vicinity of the chromophore, a *p*-hydroxybenzylidineimidazolinone group, plays a critical role in modulating the fluorescence quantum yield of the protein. Indeed, chromophore model compounds and denatured GFP fail to fluoresce appreciably except under cryogenic conditions,[5] and scrutiny of the crystal structures of different GFPs reveals important hydrogen bonds that involve the chromophore and nearby residues (e.g.,[6, 7]). In the structure of the Ser65Thr variant determined at pH 4.6, for example, the phenolic form of the chromophore appears to be hydrogen bonded to Thr203 and an internal water molecule. By comparison, at pH 8.0, the phenolate group forms an additional hydrogen bond to His148, and the protein appears to fluoresce more brightly.[8] Evidently, these interactions stabilize fluorescent forms of the chromophore, but the individual contribution of each bond to the high fluorescence of GFP remains unclear. Blue-emitting variants of the protein (i.e., BFPs) are ideal subjects to address this issue, because while replacement of Tyr66 with a His residue introduces a new hydrogen bond to Glu222, it severs all but one of the hydrogen bonds that anchors the distal ring of the chromophore in the wild-type protein. This structural simplification facilitates the correlation between pressure- or temperature-induced changes in fluorescence with the direct interaction of His66 with His148 under acidic conditions[9] or via a water molecule at pH 8.5.[10] Here, we report such a study and conclude that this interaction plays a very important role in achieving the high fluorescence exhibited by GFP-like fluoroproteins.

Materials and Methods

Sample Preparation. The gene encoding wild-type GFP in the plasmid pRSET$_b$-GFP was mutated (QuickChange, Stratagene) to replace Tyr145, Tyr66, and Ser65 with Phe, His, and Thr, respectively. All three mutations were verified by automated sequencing of the entire gene, and the protein was expressed and purified as described previously with *E. coli* BL21(DE3)::pLys.[11] After extensive dialysis to remove imidazole and free nickel ions, the protein was concentrated by ultracentrifugation (Centricon10, Millipore) and refrigerated until needed. This protein was used without further purification.

Spectroscopic Analysis. For hyperbaric measurements, 200 μL of the protein solution (1 mM BFP in 50 mM Tris buffer,

* To whom correspondence should be addressed. Phone: 650-723-4482. Fax: 650-723-4817. E-mail: sboxer@stanford.edu.

[†] Permanent address: Institute of Physics, University of Tartu, Riia 142, Tartu 51014, Estonia

[‡] Present address: Naval Research Laboratory, Washington, DC 20375.

[§] Present address: Department of Biochemistry and Molecular Biology, University of British Columbia, Vancouver, BC, Canada.

10.1021/jp0448595 CCC: $30.25
Published on Web 06/11/2005

pH 8.0) was deposited on the sapphire window of one of two coaxial optical ports of a pressure cell. The solution was sealed with a flexible, transparent, and impermeable polyethylene membrane to avoid mixing of the protein with hydraulic oil. After assembling the pressure cell, the sample was pressurized to a desired value with a hydraulic pump and pressure intensifier for analysis of the protein by absorbance and fluorescence spectroscopy as outlined below. Before advancing to the next setting, the pressure was measured again to ensure that the pressure did not drop due to oil leakage during individual measurements. Data sets were collected either with increasing pressures starting at atmospheric levels or in the reverse direction starting at the maximum pressure possible (570 MPa).

Absorption spectra of samples in the pressure cell were collected in single beam mode with light from a 300 W xenon arc lamp that was dispersed through a single grating monochromator (*f* 0.22 m; Spex Model 1681), chopped at 400 Hz for lock-in detection (Stanford Research Systems Model SR850), and focused through the optical port of the pressure cell. The transmitted light was detected with a silicon photodiode (EG&G). Signal values were recorded with LabView and subsequently converted to absorbance with a blank transmission spectrum collected in the absence of the pressure cell. The absorbance due to the hydraulic oil, sapphire windows, and polyethylene film was largely featureless in the regions of interest.

Fluorescence excitation and emission spectra were obtained with a Fluoromax 2 (Instruments S.A.) fluorimeter. The excitation and emission bandwidth used was 2 nm. The excitation beam was reflected through a port in the front of the instrument and focused with a series of lenses onto the sample that was placed ~5 cm outside of the instrument. Fluorescence was collected with the same lenses and reflected back to the analyzer of the fluorimeter. Fluorescence spectra are expressed in terms of relative quantum yield by integrating and normalizing spectra with respect to the spectrum collected at room temperature and atmospheric pressure.

To collect absorbance and fluorescence spectra as a function of temperature down to 80 K, trehalose was added to a protein solution to 10% (w/v). Drops of this solution were deposited on multiple clean quartz plates and allowed to dry overnight, resulting in ~75 μm thick films. These samples were clamped in a miniature Joule-Thompson refrigerator (MMR Technologies) that was placed outside the fluorimeter as described above or in the sample compartment of a Lambda 19 UV/vis/NIR spectrophotometer (Perkin-Elmer). Temperatures were changed gradually to the desired values. Before acquiring absorbance or fluorescence spectra, samples were incubated at a particular temperature for 3−5 min to ensure thermal equilibration and to verify that the sample remained transparent. These measurements were repeated with the protein in a 25 mM HEPES buffer solution, pH 7.9, 150 mM NaCl, and 50% glycerol (v/v) as a glassing agent to facilitate comparisons between the kinetic results obtained with trehalose (TCSPC) or in a 50% glycerol solution (fluorescence upconversion; see below).

Nanosecond and Picosecond Fluorescence Lifetimes. Fluorescence lifetimes in the subnanosecond regime were obtained with a frequency-doubled, pulse-picked, mode-locked femtosecond Ti-sapphire laser (Coherent) to provide 4.75 MHz repetition rate, 390 nm illumination. Emitted photons were selected with a D480/50 emission filter (Omega) and detected with an avalanche photodiode (EG&G) equipped with a standard, time-correlated single-photon counting device (PicoQuant, TimeHarp) to generate lifetime histograms as a function of either pressure or temperature. The instrument response of this setup was 1.1 ns, adequate for characterizing the long-lived components of the fluorescence and compatible with the geometry of the high-pressure cell.

The time evolution of fluorescence as a function of temperature was also examined during the initial 30 ps following a mode-locked excitation pulse with a fluorescence upconversion setup described previously.[12,13] Briefly, the 460 nm emission from BFP samples in the miniature Joule-Thompson refrigerator was monitored at different temperatures between 125 and 325 K. Samples were excited at 82 MHz repetition rate with 1 mW of 400 nm light polarized at the magic angle with respect to the gate beam. The instrument response function generated from the mixing of the gate beam with the scattered excitation light was typically ~140 fs. Because of the constrained geometry of the high-pressure cell, it was not possible to measure ultrafast fluorescence at high pressure by upconversion.

All lifetime data sets were analyzed by convoluting the appropriate instrument response with a model function composed of a sum of exponentials, a baseline, and a time offset.

Results

The BFP Mutation. At room temperature and atmospheric pressure, the spectroscopic properties of the Y145F/S65T/Y66H variant of GFP are typical of other GFPs where Tyr66 is replaced with a histidine residue (i.e., BFP;[1,14]). Maximal absorption is at 382 nm with a shoulder at 370 nm, and the fluorescence peaks at 445 nm with flanking shoulders at 420 and 469 nm. The fluorescence quantum yield (Φ_f) of this protein at room temperature was measured to be 0.20 in agreement with the value of 0.17 previously reported for the similar protein EBFP (F64L/S65T/Y66H/Y145F).[15] Monitoring this fluorescence in the picosecond (upconversion) and nanosecond (TCSPC) time regimes reveals multiexponential decay behavior consistent with earlier reports.[16] At least three kinetic phases were detected with lifetimes that are characterized as short- (<100 ps), intermediate- (hundreds of picoseconds), or long-lived (>2 ns). The multiexponential fluorescence decay probably stems from the excitation of different conformations of the protein and/or from the effect of multiple modes of relaxation accessible to the excited state.

Influence of Pressure on BFP. With increasing hydrostatic pressure (1−570 MPa) the absorption spectrum of BFP exhibits a small (~10%), reversible gain in intensity between 340 and 440 nm without significant shifts in the absorption maximum (not shown). This small change and reversibility are consistent with the results of Scheyhing et al., who have shown that various GFPs retain their native structure even at pressures >1000 MPa.[17] More importantly, denaturation of these proteins typically results in a loss of fluorescence, but BFP emission increases reversibly and monotonically with pressure (Figure 1). This fluorescence enhancement ($\Delta\Phi_f \sim 0.0003$ MPa^{-1}) begins at a threshold pressure of ~100 MPa, and Φ_f reaches a value of 0.34−0.36 (i.e., 75% enhancement) at the maximum attainable pressure (570 MPa). Concurrently, the vibronic structure becomes better resolved. No appreciable hysteresis is observed in the fluorescence, regardless of the direction in which pressure is changed.

Scrutiny of the timed-resolved fluorescence decay profiles of BFP collected as a function of pressure (Figure 2A) reveals that, while the lifetime of the long-lived decay component τ_{long} does not change significantly with pressure, it is primarily a growing contribution to the overall decay by this component that accounts for the increased fluorescence (Figure 2B). The

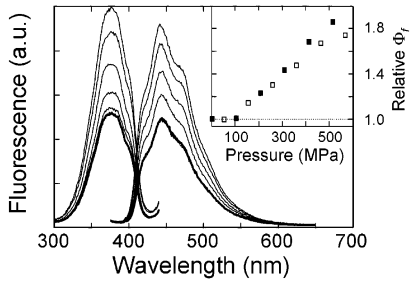

Figure 1. Pressure dependence of BFP fluorescence. Excitation (450 nm detection) and emission (360 nm excitation) spectra of a BFP sample (50 mM Tris buffer, pH 8.0) were acquired at atmospheric pressure (bold spectra of lowest intensity) and again at 103, 207, 310, 414, and 517 MPa. Excitation and emission spectra were collected with 2 nm bandwidth. Inset: Quantum yield of fluorescence, relative to BFP at atmospheric pressure, calculated from these emission spectra. The filled and open squares represent the fluorescence measured as a function of decreasing and increasing pressure, respectively.

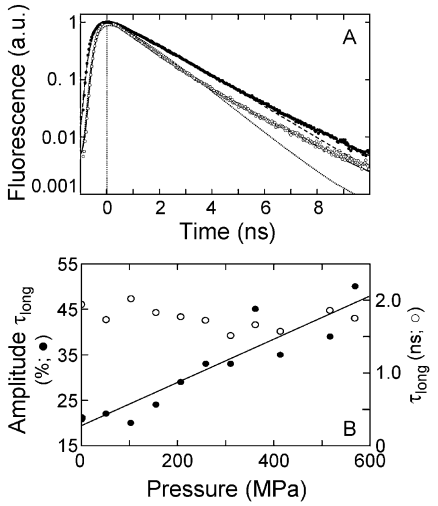

Figure 2. (A) Comparison of the time-resolved BFP fluorescence decay [390 nm excitation, 480 nm (50 nm fwhh) emission] at atmospheric pressure (open circle) and at 569 MPa (filled circle). The dotted and dashed curves represent a fit of these data to a monoexponential decay model, and the solid curves represent a fit of the same data to a biexponential process. (B) Summary of the influence of pressure on the fluorescence decay of BFP. The open and filled circles represent the lifetime and amplitude change associated with the long-lived component as determined from a fit of each decay profile to a multiexponential decay process.

short and intermediate components account for less of the fluorescence decay so it is difficult to assess whether the lifetimes of these phases change significantly.

Effect of Cryogenic Temperatures on BFP. A fluorescence enhancement equivalent to that observed at 570 MPa can be elicited also by freezing BFP in a trehalose film to just ~270 K (Figure 3). Decreasing the temperatures further results in greater fluorescence enhancement so that by ~125 K, Φ_f is 4.5-fold greater than it is at room temperature. Interestingly, this temperature dependence (Figure 3 inset) can be fit with two linear segments that intersect at ~205 K, which is in the region of what is regarded generally as the "slaved" glass transition temperature of proteins (T_g, vide infra[18,19]). In contrast, the absorbance of BFP increases modestly (~7%) with a negligible shift of the principal absorption band to longer wavelength (2−3 nm; data not shown). These small changes in the absorption spectrum suggest that the ground and first excited singlet states of the chromophore are either largely unperturbed under the conditions of the experiment or they changed essentially in the same way. In either case, the large increase in emission observed cannot be accounted for by the slight change in absorption cross section.

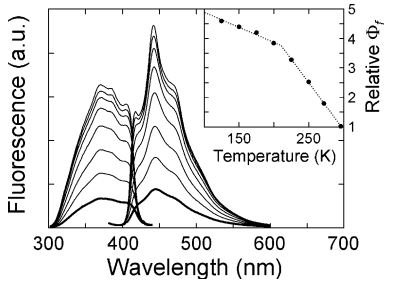

Figure 3. Emission (360 nm excitation) and excitation (450 nm detection) spectra of a BFP sample (50 mM Tris buffer, pH 8.0, in a 10% trehalose matrix) collected as a function of temperature with 2 nm excitation and emission bandwidths. Fluorescence intensity increased sequentially with decreasing temperature starting at room temperature (bold spectra of lowest intensity), 272, 250, 225, 200, 275, 250, and 125 K. Inset: Plot of the fluorescence quantum yield of BFP (relative to Φ_f at 296 K) as a function of temperature. The interpolated linear segments (dotted lines) intersect at 205 K.

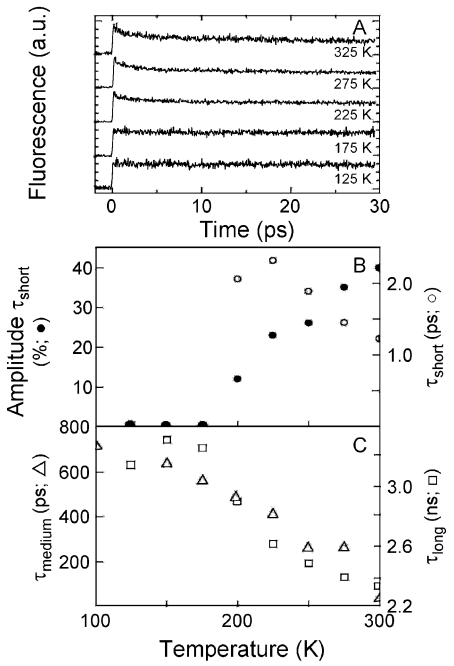

Figure 4. (A) Comparison of the time-resolved fluorescence decay of BFP excited at 400 nm and the resulting 460 nm emission as monitored by fluorescence upconversion during the first 30 ps at the temperatures indicated. (B) Summary of the effect of temperature on the amplitude contribution (filled circle) and lifetime (open circle) of the shortest detectable decay component of BFP fluorescence, as measured by TCSPC. (C) Summary of the effect of temperature on the lifetimes of intermediate- and long-lived components of BFP fluorescence excited with 390 nm light, as measured by TCSPC.

Figure 4A illustrates the time-resolved fluorescence decay of BFP monitored in the picosecond regime and at temperatures down to 125 K. Analysis of these data reveals that τ_{short} becomes an increasingly minor component of the decay at lower temperatures and is undetectable below ~175 K (Figure 4B). At longer time scales, the increasingly monoexponential character of the fluorescence decay with decreasing temperature is also evident from the growing contribution of the long-lived components to the overall decay of BFP fluorescence. At the same time, their lifetime increases substantially (Figure 4C).

Discussion

Model compounds of the *p*-hydroxybenzylideneimidazolinone group are virtually nonfluorescent in alcohol solutions at room temperature ($\Phi_f < 10^{-3}$), but their emission increases ~1000-fold when cooled to 77 K.[20] This enhancement is associated with prolonged fluorescence lifetimes as has been shown with the model compound ethyl 4-(4-hydroxyphenyl)methylidene-2-methyl-5-oxo-1-imidazolacetate,[21] suggesting that chromophore mobility facilitates rapid internal conversion, leading to conical intersections of the ground and excited-state energy surfaces and, thus, to efficient relaxation of the excited state via one or more nonradiative pathways. However, the weak dependence of fluorescence on solvent viscosity above the supercooled fluid or glass regimes argues that large-scale intramolecular rearrangement of the chromophore (i.e., cis−trans isomerization) is not strictly necessary to reduce radiative decay so dramatically. Instead, results from molecular dynamics simulations indicate that a volume-conserving rotation about the dihedral angles φ and τ of the ground-state chromophore of up to $\pm 7°$ is generally the greatest deviation from coplanarity between the phenolic and imidazolinone rings inside the confines of the protein,[22] suggesting that only relatively small motions of the chromophore are permitted by the cavity.[23]

Whether or not rotations of this magnitude are sufficient to compete with GFP fluorescence as a mode of relaxation remains to be proven, because the protein could also exert a strong influence on the electronic structure of the chromophore to suppress internal conversion. Follenius-Wund et al., for example, investigated a diverse set of imidazolone compounds with Φ_f ranging from 10^{-4} to 0.258 in solution.[24] The emission of these compounds was enhanced significantly in low dielectric solvents such as dioxane ($\epsilon = 2.2$), suggesting that the role of the surrounding protein is not only to constrain the motions of the chromophore but also to provide a less polar environment. Nevertheless, semiempirical calculations on the electronic ground and excited states of these molecules confirmed that the crucial variable in determining the fluorescence quantum yield is freedom of rotation about the bonds that connect the rings of the chromophore. Therefore, it is interesting to note that the low $\Phi_f \sim 0.2$ exhibited by BFP correlates with the facts that His66 does not profit from the intricate hydrogen-bond network that Tyr66 does in the wild-type sequence[9] and the chromophore cavity does not shrink appreciably to fill-in the space left vacant as a result of the amino acid replacement.[9]

The pressure-linked fluorescence enhancement exhibited by BFP parallels the response of the wild-type protein and of other variants when these are subjected to comparable conditions.[25] Unlike the situation with these other fluoroproteins, however, BFP fluorescence can probably increase further with increasing pressure because of its relatively lower Φ_f at 1 atm and because the structure of GFPs appears to be generally stable up to at least ~800−1300 MPa.[17,26] Nevertheless, the similar effect of elevated hydrostatic pressures on these proteins suggests that the origin of fluorescence enhancement is common to these proteins, regardless of mutations that might affect other characteristics, such as the emission wavelength.

A picture emerging from recent investigations on the compressibility of globular proteins is that cavities within these proteins shrink and often hydrate in response to increasing hydrostatic pressures. At the same time, side-chain dynamics decrease, particularly at the protein surface as conformational equilibria shift toward structures of smaller volume.[27] From a survey of experimental data gathered with a variety of techniques, it appears that the typical isothermal compressibility coefficient for a protein is $\sim(1-2) \times 10^{-4}$ MPa^{-1}.[28] Neglecting higher order effects, this value translates into a decrease in the volume of BFP of ~ 9% at 570 MPa. This contraction is achieved in the chromophore cavity by a shortening of distances between atoms that are not bound covalently of ~3% that would, in turn, facilitate the formation of hydrogen bonds between the chromophore and neighboring residues (e.g., His148; PDB ID 1BFP[9] or 2EMO[10]) and water molecules (e.g., HOH305; PDB ID 1EMF[10]). Existing interactions would similarly increase in strength[29] with the end result being that chromophore mobility is reduced. Thus, an increase in fluorescence intensity is associated with fewer conformational states available for the chromophore to sample; the increasingly monoexponential character of the fluorescence decays observed at high pressures is consistent with this premise.

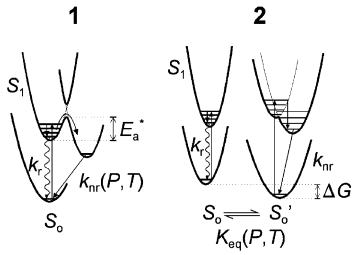

Figure 5. Proposed schemes that illustrate how the BFP chromophore's pressure- and temperature-dependent rate of conversion to a nonfluorescent state can affect the populations of emitting and nonemitting species, according to eqs 1 and 2.

Analysis of the temperature dependence of the fluorescence and its multiexponential decay suggests that the chromophore in BFP exhibits significant structural fluctuations at room temperature with one or more conformations (likely many, given the multiexponential fluorescence decay at room temperature) decaying nonradiatively back to the ground state (Figure 5). The contribution of the various decay processes to Φ_f is thus a function of the radiative and nonradiative rate constants for these processes (k_r and k_{nr}, respectively) according to eq 1

$$\Phi_f = \frac{k_r}{k_r + k_{nr}} \tag{1}$$

Reformulating eq 1 as an Arrhenius expression (eq 2),

$$k_{nr}(T) = k_r\left(\frac{1 - \Phi_f(T)}{\Phi_f(T)}\right) = A' \exp\left(\frac{-E_a^*}{RT}\right) \tag{2}$$

where A' and R are a preexponential factor and the gas constant, respectively, and T is the absolute temperature, yields an activation energy (E_a^*) that is associated with the interconversion between fluorescent and nonfluorescent states of the chromophore (case 1, Figure 5). This treatment is justified because τ_{long} and the integrated absorption remain largely invariant with temperature, and therefore it is reasonable to attribute the changes in Φ_f to more significant changes in the nonradiative decay. An Arrhenius plot of the log of eq 2 versus the reciprocal of temperature is shown in Figure 6. As seen earlier (Figure 3 inset), these data delineate two linear segments that intersect at $T_g^{-1} \sim 0.005$ K^{-1}. At $T > T_g$ (~200 K) protein structures undergo higher amplitude fluctuations generally believed to be necessary for their function.[18,19] Therefore, it is noteworthy that the fluorescence observed in this temperature range (i.e., the steeper line segment in Figure 6) is associated with an activation energy of 18.7 kJ/mol, because this value

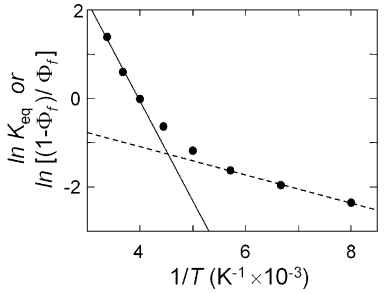

Figure 6. Arrhenius plot of the BFP fluorescence enhancement. The activation energies associated with BFP fluorescence enhancement are 18.7 and 2.6 kJ/mol, respectively, for the segments interpolated with the solid and dashed lines. Lower limits for the entropy and enthalpy associated with the enhanced fluorescence observed above the glass regime were estimated from the solid line shown. The thermodynamic parameters have values of −75 J/mol/K and −19 kJ/mol, respectively.

coincides with the reported hydrogen-bond energy for His dimer formation.[30−32] In the crystal structure of BFP, the imidazole ring of the chromophore makes a weak (∼3.1 Å at 295 K) hydrogen bond with His148;[9] consequently, it appears that as the temperature is reduced, the chromophore is increasingly immobilized as this hydrogen bond, or a linkage mediated by a water molecule becomes stronger. At the other extreme (i.e., $T < T_g$), harmonic vibrations of less mobile subconformations probably constitute the dominant motions that remain. Consequently, the fluorescence enhancements elicited below 200 K ($E_a^* = 2.6$ kJ/mol) are probably related to a low energy barrier that restricts twisting motions in the electronically excited state of the chromophore.

An alternative mechanism that could explain the observed fluorescence increase would postulate multiple ground state conformations of the chromophore at equilibrium, the excited state of at least one of which decays nonradiatively (case 2, Figure 5). Equilibrium constants (K_{eq}) for the interconversion between fluorescent, hydrogen-bonded states of the chromophore and nonfluorescent forms were calculated on the basis of a Φ_f value of 0.20 at 298 K to estimate the thermodynamic parameters associated with this conformational equilibrium. Between 298 and 250 K, the entropy and enthalpy contributions are ca. −75 J/mol/K and −19 kJ/mol, respectively (Figure 6). These values probably represent a lower limit because the interpretation of the results is simplified here as a two-state process (i.e., fluorescent ⇔ nonfluorescent). Nevertheless, it appears that this conformational conversion is entropy-driven at temperatures above ∼250 K but enthalpy-driven at lower temperatures. Qualitatively, this conclusion is consistent with the greater structural mobility expected at temperatures $> T_g$, where His66 in BFP is relatively free to explore multiple subconformations, and with the multiexponential fluorescence decay observed at room temperature.

A more complete description of the mechanism(s) at play here is likely some combination of the limiting situations depicted by cases 1 and 2 in Figure 5. Even so, it appears that a key factor that determines whether the protein will fluoresce is the hydrogen-bond network of the phenolic oxygen atom of the chromophore (or the imidazole nitrogen in the BFP variant of this work) that helps maintain this group in a planar conformation. This observation is supported by the work of Lukyanov and co-workers, who successfully transformed GFP-like "chromoproteins" from a number of *Anthozoan* species into fluoroproteins by introducing amino acids into the chromophore cavity that can hydrogen bond with this group.[33] Concomitantly, the replacement of similar residues in *Ds*Red to ensure that the monomer matures into a red-emitting form (e.g., Lys163) results in a drop in the fluorescence quantum yield by 20%.[34] Our data show that the equilibrium between hydrogen-bonded and nonbonded chromophores stems from the balance between entropy and enthalpy factors to account for substantial radiative decay.

Acknowledgment. The authors are indebted to the late Prof. H. G. Drickamer for the loan of the pressure cell used in these experiments and thank Prof. Curtis Franck for the use of a pressure intensifier. This material is based upon work supported by the National Science Foundation under Grant No. MCB-9816947 and MCB-0212503 (W.E.M.) and by the National Institutes of Health under Grant No. GM27738 (S.G.B.). K.M. was the grateful recipient of a Fulbright Fellowship and appreciates the support from the Estonian Science Foundation Grant 5546. F.I.R. gratefully acknowledges a Postdoctoral Fellowship from the Natural Sciences and Engineering Research Council of Canada.

References and Notes

(1) Tsien, R. Y. *Annu. Rev. Biochem.* **1998**, *67*, 509.
(2) Zimmer, M. *Chem. Rev.* **2002**, *102*, 759.
(3) Wang, L.; Xie, J.; Deniz, A. A.; Schultz, P. G. *J. Org. Chem.* **2003**, *68*, 174.
(4) Bae, J. H.; Rubini, M.; Jung, G.; Wiegand, G.; Seifert, M.; Azim, M. K.; Kim, J.-S.; Zumbusch, A.; Holak, T. A.; Moroder, L.; Huber, R.; Budisa, N. *J. Mol. Biol.* **2003**, *328*, 1071.
(5) Niwa, H.; Inouye, S.; Hirano, T.; Matsuno, T.; Kojima, S.; Kubota, M.; Ohashi, M.; Tsuji, F. I. *Proc. Natl. Acad. Sci. U.S.A.* **1996**, *93*, 13617.
(6) Brejc, K.; Sixma, T. K.; Kitts, P. A.; Kain, S. R.; Tsien, R. Y.; Ormo, M.; Remington, S. J. *Proc. Natl. Acad. Sci. U.S.A.* **1997**, *94*, 2306.
(7) Yang, F.; Moss, L. G.; Phillips, G. N., Jr. *Nat. Biotechnol.* **1996**, *14*, 1246.
(8) Elsliger, M. A.; Wachter, R. M.; Hanson, G. T.; Kallio, K.; Remington, S. J. *Biochemistry* **1999**, *38*, 5296.
(9) Wachter, R. M.; King, B. A.; Heim, R.; Kallio, K.; Tsien, R. Y.; Boxer, S. G.; Remington, S. J. *Biochemistry* **1997**, *36*, 9759.
(10) Palm, G. J.; Zdanov, A.; Gaitanaris, G. A.; Stauber, R.; Pavlakis, G. N.; Wlodawer, A. *Nat. Struct. Biol.* **1997**, *4*, 361.
(11) Lounis, B.; Deich, J.; Rosell, F. I.; Boxer, S. G.; Moerner, W. E. *J. Phys. Chem. B* **2001**, *105*, 5048.
(12) Stanley, R. J.; Boxer, S. G. *J. Phys. Chem.* **1995**, *99*, 859.
(13) Chattoraj, M.; King, B. A.; Bublitz, G. U.; Boxer, S. G. *Proc. Natl. Acad. Sci. U.S.A.* **1996**, *93*, 8362.
(14) Heim, R.; Prasher, D. C.; Tsien, R. Y. *Proc. Natl. Acad. Sci. U.S.A.* **1994**, *91*, 12501.
(15) Patterson, G. H.; Knobel, S. M.; Sharif, W. D.; Kain, S. R.; Piston, D. W. *Biophys. J.* **1997**, *73*, 2782.
(16) Lossau, H.; Kummer, A.; Heinecke, R.; Poellinger-Dammer, F.; Kompa, C.; Bieser, G.; Jonsson, T.; Silva, C. M.; Yang, M. M. *Chem. Phys.* **1996**, *213*, 1.
(17) Scheyhing, C. H.; Meersman, F.; Ehrmann, M. A.; Heremans, K.; Vogel, R. F. *Biopolymers* **2002**, *65*, 244.
(18) Iben, I. E. T.; Braunstein, D.; Doster, W.; Frauenfelder, H.; Hong, M. K.; Johnson, J. B.; Luck, S.; Ormos, P.; Schulte, A. *Phys. Rev. Lett.* **1989**, *62*, 1916.
(19) Reat, V.; Dunn, R.; Ferrand, M.; Finney, J. L.; Daniel, R. M.; Smith, J. C. *Proc. Natl. Acad. Sci. U.S.A.* **2000**, *97*, 9961.
(20) Webber, N. M.; Litvinenko, K. L.; Meech, S. R. *J. Phys. Chem. B* **2001**, *105*, 8036.
(21) Kummer, A. D.; Kompa, C.; Niwa, H.; Hirano, T.; Kojima, S.; Michel-Beyerle, M. E. *J. Phys. Chem. B* **2002**, *106*, 7554.
(22) Helms, V.; Straatsma, T. P.; McCammon, J. A. *J. Phys. Chem. B* **1999**, *103*, 3263.
(23) Chen, M. C.; Lambert, C. R.; Urgitis, J. D.; Zimmer, M. *Chem. Phys.* **1999**, *270*, 157.
(24) Follenius-Wund, A.; Bourotte, M.; Schmitt, M.; Iyice, F.; Lami, H.; Bourguignon, J.-J.; Haiech, J.; Pigault, C. *Biophys. J.* **2003**, *85*, 1839.
(25) Ehrmann, M. A.; Scheyhing, C. H.; Vogel, R. F. *Lett. Appl. Microbiol.* **2001**, *32*, 230.
(26) Herberhold, H.; Marchal, S.; Lange, R.; Scheyhing, C. H.; Vogel, R. F.; Winter, R. *J. Mol. Biol.* **2003**, *330*, 1153.
(27) Akasaka, K. *Pure Appl. Chem.* **2003**, *75*, 927.
(28) Kharakoz, D. P. *Biophys. J.* **2000**, *79*, 511.
(29) Czeslik, C.; Jonas, J. *Chem. Phys. Lett.* **1999**, *302*, 633.

(30) Zimmermann, H. *Z. Elektrochem. Angew. Phys. Chem.* **1961**, *65*, 821.
(31) Link, K. H.; Grimm, H.; Dorner, B.; Zimmermann, H.; Stiller, H.; Bleckmann, P. *J. Phys. Chem. Solids* **1985**, *46*, 135.
(32) Wang, F.-F. C.; Hirs, C. H. W. *J. Biol. Chem.* **1979**, *254*, 1090.
(33) Gurskaya, N. G.; Savitsky, A. P.; Yanushevich, Y. G.; Lukyanov, S. A.; Lukyanov, K. A. *BMC Biochem.* **2001**, *2*, 6.
(34) Campbell, R. E.; Tour, O.; Palmer, A. E.; Steinbach, P. A.; Baird, G. S.; Zacharias, D. A.; Tsien, R. Y. *Proc. Natl. Acad. Sci. U.S.A.* **2002**, *99*, 7877.